



Incipient piezoelectrics and electrostriction behavior in Sn-doped $\text{Bi}_{1/2}(\text{Na}_{0.82}\text{K}_{0.18})_{1/2}\text{TiO}_3$ lead-free ceramics

Hyoung-Su Han, Wook Jo, Jin-Kyu Kang, Chang-Won Ahn, Ill Won Kim, Kyoung-Kwan Ahn, and Jae-Shin Lee

Citation: *Journal of Applied Physics* **113**, 154102 (2013); doi: 10.1063/1.4801893

View online: <http://dx.doi.org/10.1063/1.4801893>

View Table of Contents: <http://scitation.aip.org/content/aip/journal/jap/113/15?ver=pdfcov>

Published by the [AIP Publishing](#)

Articles you may be interested in

Electric-field-temperature phase diagram of the ferroelectric relaxor system $(1-x)\text{Bi}_{1/2}\text{Na}_{1/2}\text{TiO}_3-x\text{BaTiO}_3$ doped with manganese

J. Appl. Phys. **115**, 194104 (2014); 10.1063/1.4876746

Electromechanical strain and bipolar fatigue in $\text{Bi}(\text{Mg}_{1/2}\text{Ti}_{1/2})\text{O}_3-(\text{Bi}_{1/2}\text{K}_{1/2})\text{TiO}_3-(\text{Bi}_{1/2}\text{Na}_{1/2})\text{TiO}_3$ ceramics

J. Appl. Phys. **114**, 054102 (2013); 10.1063/1.4817524

Switching of morphotropic phase boundary and large strain response in lead-free ternary $(\text{Bi}_{0.5}\text{Na}_{0.5})\text{TiO}_3-(\text{K}_{0.5}\text{Bi}_{0.5})\text{TiO}_3-(\text{K}_{0.5}\text{Na}_{0.5})\text{NbO}_3$ system

J. Appl. Phys. **113**, 114106 (2013); 10.1063/1.4795511

Electrostrictive effect in lead-free relaxor $\text{K}_{0.5}\text{Na}_{0.5}\text{NbO}_3-\text{SrTiO}_3$ ceramic system

J. Appl. Phys. **98**, 024113 (2005); 10.1063/1.1989438

Relaxorlike dielectric properties and history-dependent effects in the lead-free $\text{K}_{0.5}\text{Na}_{0.5}\text{NbO}_3-\text{SrTiO}_3$ ceramic system

Appl. Phys. Lett. **85**, 994 (2004); 10.1063/1.1779947

A wide orange banner with a white border. The text '2014 Special Topics' is centered in a large, white, sans-serif font. Below the text are five circular icons, each containing a different material structure and a label: 'PEROVSKITES' (red and black geometric shapes), '2D MATERIALS' (blue and red grid), 'MESOPOROUS MATERIALS' (green and blue porous structure), 'BIOMATERIALS/ BIOELECTRONICS' (yellow and black grid), and 'METAL-ORGANIC FRAMEWORK MATERIALS' (brown and black porous structure). At the bottom left is the 'AIP | APL Materials' logo. At the bottom right is a red ribbon with the text 'Submit Today!' in white.

2014 Special Topics

PEROVSKITES

2D MATERIALS

MESOPOROUS MATERIALS

BIOMATERIALS/ BIOELECTRONICS

METAL-ORGANIC FRAMEWORK MATERIALS

AIP | APL Materials

Submit Today!

Incipient piezoelectrics and electrostriction behavior in Sn-doped $\text{Bi}_{1/2}(\text{Na}_{0.82}\text{K}_{0.18})_{1/2}\text{TiO}_3$ lead-free ceramics

Hyoung-Su Han,¹ Wook Jo,² Jin-Kyu Kang,¹ Chang-Won Ahn,³ Ill Won Kim,³ Kyoung-Kwan Ahn,⁴ and Jae-Shin Lee^{1,a)}

¹*School of Materials Science and Engineering, University of Ulsan, Ulsan, South Korea*

²*Institute of Materials Science, Technische Universität Darmstadt, Petersenstrasse 23, 64287 Darmstadt, Germany*

³*Department of Physics, University of Ulsan, Ulsan, South Korea*

⁴*School of Mechanical Engineering, University of Ulsan, Ulsan, South Korea*

(Received 15 March 2013; accepted 1 April 2013; published online 17 April 2013)

Dielectric, ferroelectric, piezoelectric, and strain properties of lead-free Sn-doped $\text{Bi}_{1/2}(\text{Na}_{0.82}\text{K}_{0.18})_{1/2}\text{TiO}_3$ (BNKT) were investigated. A crossover from a nonergodic relaxor to an ergodic relaxor state at room temperature, accompanied by a giant electric-field-induced strain, was observed at 5 at. % Sn doping. Switching dynamics monitored during a bipolar poling cycle manifested that the observed giant strain originates from incipient piezoelectricity. When Sn doping level reached 8 at. %, BNKT exhibited an electrostrictive behavior with a highly temperature-insensitive electrostrictive coefficient of $Q_{11} = 0.023 \text{ m}^4 \text{ C}^{-2}$. © 2013 AIP Publishing LLC
[\[http://dx.doi.org/10.1063/1.4801893\]](http://dx.doi.org/10.1063/1.4801893)

I. INTRODUCTION

Lead-free perovskite piezoceramics have been extensively studied as alternatives to lead-containing counterparts since the environmental regulations on harmful elements was in effect.^{1,2} Since a giant electric-field-induced strain was reported by Zhang *et al.*³ in $\text{Bi}_{1/2}\text{Na}_{1/2}\text{TiO}_3\text{-BaTiO}_3\text{-(K}_{1/2}\text{Na}_{1/2})\text{NbO}_3$ (BNT-BT-KNN) ceramics, great attention has been paid to $(\text{Bi}_{1/2}\text{Na}_{1/2})\text{TiO}_3$ (BNT)-based perovskite ceramics in expectation for large-stroke actuator applications such as fuel injectors and vacuum circuit breakers. A common strategy so far was to incorporate a small amount of additional chemical entities such as single isovalent dopants,^{4,5} donors,^{6,7} or ABO_3 -type compounds^{8–10} into BNT-BT or BNT- $(\text{Bi}_{1/2}\text{K}_{1/2})\text{TiO}_3$ (BKT) solid solution systems at the so-called morphotropic phase boundary (MPB).^{11,12} Here, we use the term, giant strains, to distinguish them from the conventional electric-field-induced strain in poled ferroelectric (FE) materials in that the onset of these strains requires a certain threshold electric field level (referred to as E_{pol} hereafter), but this electric-field-induced poling state becomes unstable with little trace of perceivable piezoelectricity when the field is removed.^{13,14} This phenomenological feature categorized the materials with such strain behavior as a new material class designated as incipient piezoceramics.¹⁵

In spite of the exceptionally large strains available in the incipient piezoceramics, there are at least three challenges to be overcome for versatile applications. One is a relatively large electric field required for activating the giant strains. For the piezoelectric components to be incorporated into devices, the giant strain should be inducible within the limit of operating voltage allowed for the devices; hence, smaller driving fields are always preferable. Another challenge is

significant hysteresis in the giant strain, which is often considered as a drawback in extending the practicability of the material systems.¹⁶ The other is a rather strong temperature dependence of strain properties, e.g., $S_{\text{max}}/E_{\text{max}}$, which decreases significantly up to $\sim 150^\circ\text{C}$ for the reported materials.^{17,18} It was shown that this temperature dependence can be circumvented when only the electrostrictive part of the strain is utilized by suppressing the field-induced phase transition throughout the temperature range of interest.¹⁹ All the aforementioned challenges converge to a conclusion that the key to resolving the issues is to understand the nature of the reversible field-induced phase transition.

It is interesting to notice that the incipient piezoelectricity in BNT-BT or BNT-BKT systems have been reported to be induced by the addition of 2–3 mol. % of additional component regardless of the kind of the dopants.¹⁵ However, a recent study revealed that the development of the incipient piezoelectricity was especially retarded when isovalent Sn was introduced though other isovalent dopants such as Zr have little retarding effect.²⁰ This implies that understanding this exceptional behavior can bring us a deeper insight into the mechanism for the incipient piezoelectricity. In this study, therefore, we investigated the effect of Sn-doping on the piezoelectric, FE, crystal structure, and dielectric properties of 0.82BNT-0.18BKT. A special focus was put on the field- and temperature-dependent phase transition dynamics.

II. EXPERIMENTAL PROCEDURE

Ceramic powders conforming to the chemical formula $\text{Bi}_{1/2}(\text{Na}_{0.82}\text{K}_{0.18})_{1/2}(\text{Ti}_{1-x}\text{Sn}_x)\text{O}_3$ (BNKT_xSn), where $x = 0, 0.02, 0.05, \text{ and } 0.08$, were synthesized using a conventional solid-state reaction route. Reagent grade Bi_2O_3 , Na_2CO_3 , K_2CO_3 , SnO_2 , and TiO_2 (99.9%, High Purity Chemicals, Japan) powders were used as raw materials. These raw materials were first put in a drying oven at 100°C for 24 h to

^{a)}Author to whom correspondence should be addressed. Electronic mail: jslee@ulsan.ac.kr. Tel.: +82 52 259 2286.

remove moisture and then weighed according to the stoichiometric formula. The powders were ball-milled in ethanol with zirconia balls for 24 h, dried at 80 °C for 24 h, and calcined at 850 °C for 2 h in a covered alumina crucible. After calcination, the powder was mixed with polyvinyl alcohol (PVA) as a binder and then pressed into green discs with a diameter of 12 mm under a uniaxial pressure of 98 MPa. These green pellets were sintered at 1175 °C in a covered alumina crucible for 2 h in air.

The crystal structure of the sintered samples was characterized by X-ray diffraction (XRD, RAD III, Rigaku, Japan). For electrical measurements, a silver paste was screen-printed on both sides of specimens and subsequently burnt in at 700 °C for 30 min. The polarization (P) and strain (S) hysteresis as a function of external electric field (E) were measured at 300 mHz with a 15 μ F measurement capacitance using a Sawyer-Tower circuit equipped with an optical sensor (Philtec, Inc., Annapolis, MD, USA). The small-signal field excitation to monitor the contributions of reversible entities to $d_{33}(E)$ and $\epsilon_{33}(E)$ was measured in a commercial apparatus, aixPES (aixACCT Systems GmbH, Aachen, Germany), by applying a sinusoidal bipolar signal of 10 V/mm at 1 kHz, which was superimposed on a bipolar electric field profile with an amplitude of 6 kV/mm at 300 mHz. The temperature-dependent dielectric constant (ϵ_r) and dielectric loss ($\tan \delta$) of the poled BNKT x Sn ceramics were recorded using an impedance analyzer (HP4192A) attached to a programmable furnace at the measurement frequencies of 1–100 kHz in a temperature range of 25–550 °C.

III. RESULTS AND DISCUSSION

X-ray diffraction patterns of the BNKT x Sn ceramics are shown in Fig. 1. Careful observation indicates that undoped BNKT has a peak splitting at $\sim 46^\circ$, corresponding to the (002)/(200) reflection of a tetragonal phase.²¹ Similar to the changes in X-ray diffraction patterns for BNT-BT-KNN,³ Sn-doped BT,²² BiScO₃-Bi(Zn_{0.5}Ti_{0.5})O₃-BaTiO₃ (BS-BZT-BT),²³ BaTiO₃-BiYbO₃ (BT-BY),²⁴ and modified BNKT ceramic systems,^{4–10} the increase in Sn concentration causes the tetragonal (002)/(200) peaks to gradually merge into a single (200)_{pc} (the subscript “pc” denotes pseudocubic Miller index) reflection at $x = 0.08$, indicative of the loss of macroscopically conceivable non-cubic distortion. The trend is consistent with the previous results as shown in the BNT-BKT system with other chemical modifiers.^{9,20,25}

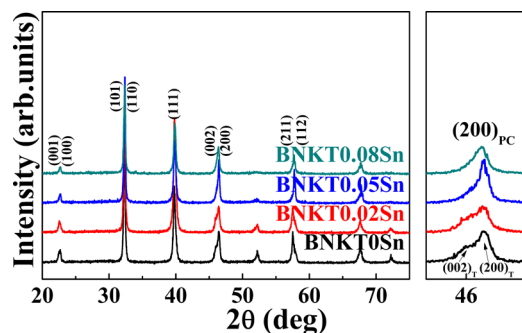


FIG. 1. X-ray diffraction patterns of Sn-doped BNKT ceramics as a function of Sn concentration.

Electric field-induced polarization and strain hysteresis loops of the BNKT x Sn ceramics are presented in Figs. 2(a) and 2(b), respectively. All the characteristic parameters such as the maximum polarization (P_{\max}), the poling strain (S_{pol}), the remanent polarization (P_{rem}), and the remanent strain (S_{rem}) decrease with increasing x , indicating that the addition of Sn suppresses a field-induced FE order, which conforms to the previous observations in modified BNKT systems.^{4–10} It is seen that there happens a significant increase in ($S_{\text{pol}} - S_{\text{rem}}$) at $x = 0.05$, beyond which it decreases drastically. The value of ($S_{\text{pol}} - S_{\text{rem}}$) corresponds to the maximum available strain (S_{max}) when the material is used as electromechanical actuator. This giant strain is activated above a certain threshold electric field involving a considerably large hysteresis^{3,26} and is only available when macroscopic piezoelectricity nearly vanishes.^{3,26} At this point, the typical butterfly-shaped strain hysteresis transforms into a sprout-shaped one, implying the destabilization of ferroelectricity at zero field.¹⁵ This categorizes the Sn-doped BNT-BKT materials as incipient piezoceramics in that the material is not macroscopically piezoelectric but evolves into one on the application of electric field. The key parameters from strain hysteresis loops are given as a function of Sn content in Fig. 3.

Figure 4 shows the temperature dependence of dielectric permittivity (ϵ_r) and dielectric loss ($\tan \delta$) for both unpoled and poled BNKT x Sn for three measurement frequencies of 1, 10, 100 kHz. All the unpoled specimens show strong frequency dispersion from room temperature up to $\sim 150^\circ\text{C}$, which suggests that all specimens can be classified as relaxor

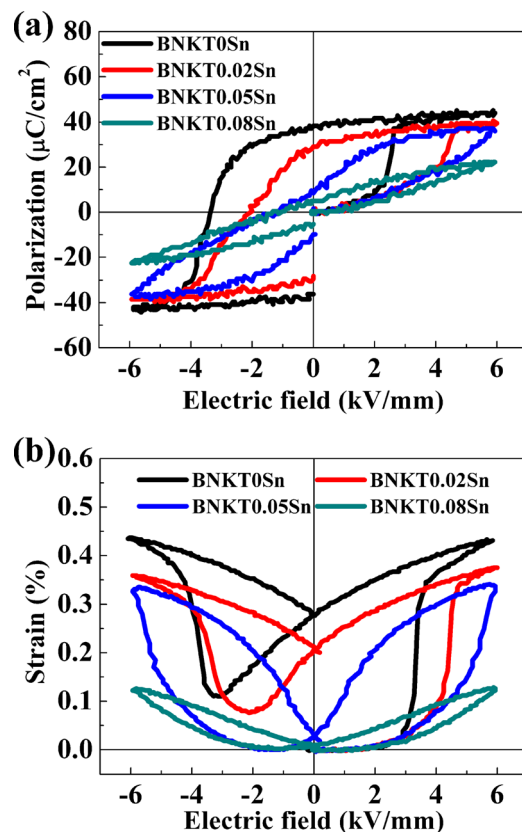


FIG. 2. $P(E)$ and $S(E)$ hysteresis loops at room temperature for Sn-doped BNKT ceramics.

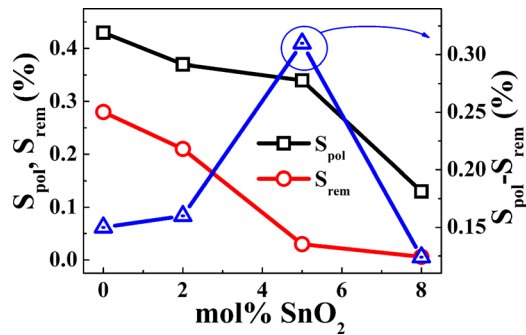


FIG. 3. Changes in S_{pol} , S_{rem} , and the difference between them ($S_{pol} - S_{rem}$) as a function of Sn concentration.

ferroelectrics. There are two distinct anomalies evident in ϵ_r for all compositions: a shoulder at $\sim 150^\circ\text{C}$ with a strong frequency dispersion and frequency-insensitive peaks at $\sim 300^\circ\text{C}$. The magnitude of overall dielectric signal is seen to decrease with increasing Sn content, while the temperature range for each anomaly remains practically invariant. Consistent observation has been reported in BT-BY,²⁴ BNT-BT,²⁷ and BNT-BKT²⁸ systems with additional chemical modifiers being introduced. On the other hand, an additional dielectric anomaly appears when the materials are electrically poled. This anomaly is commonly referred to as depolarization temperature (T_d) where a field-induced FE order converts back to an ergodic relaxor state.¹⁵ This anomaly is best seen in BNKT0Sn, manifested as a frequency independent discontinuity both in ϵ_r and $\tan \delta$. It is also seen that T_d decreases from $\sim 132^\circ\text{C}$ for BNKT0Sn to $\sim 84^\circ\text{C}$ for BNKT0.02Sn and then is not detectable for the compositions with higher Sn contents. The absence of apparent T_d in BNKT0.05Sn and BNKT0.08Sn in the current measurement data is indicative of the lowering of T_d below the room temperature by the addition of Sn.¹⁷ However, it is noticed that the electrical poling still has an influence on the dielectric

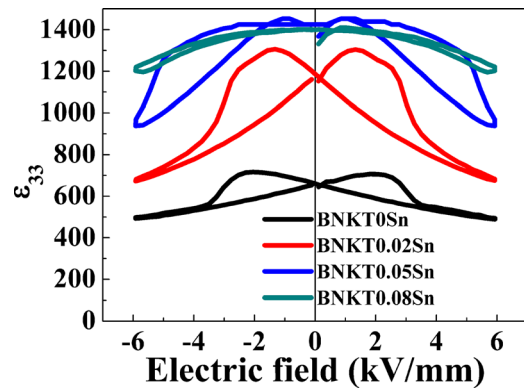


FIG. 5. Small signal $\epsilon_{33}(E)$ measured at 1 kHz of BNKT x Sn as a function of electric field.

signal even for the BNKT0.05Sn and BNKT0.08Sn, represented as a fluctuation in the spectra around 100°C . This suggests that there should still be a trace of nonergodicity in BNKT0.05Sn and BNKT0.08Sn.²⁹

The small-signal dielectric permittivity $\epsilon_{33}(E)$ of BNKT x Sn ceramics as a function of electric field is presented in Fig. 5. A significant change in the shape profile of $\epsilon_{33}(E)$ is evident with increasing Sn content, which is consistent with those observed in BZT-modified BNT-BKT.³⁰ The observed hysteresis in $\epsilon_{33}(E)$ for undoped BNKT resembles that of ordinary FE materials, representatively PZT, where the local maximum in ϵ_{33} appears near the coercive field due to field-induced domain reorientations.³¹ This means that BNKT0Sn is a nonergodic relaxor that transforms irreversibly into a FE by poling process.³² On the other hand, with 2 at. % doping of Sn, two distinct features are noticed. One is a significant increase in the absolute value of $\epsilon_{33}(E)$ at zero field, which could be attributed either to an increased mobility of polar nanoregions (PNRs) or to an increase in their density. The other is a splitting in local maxima, both

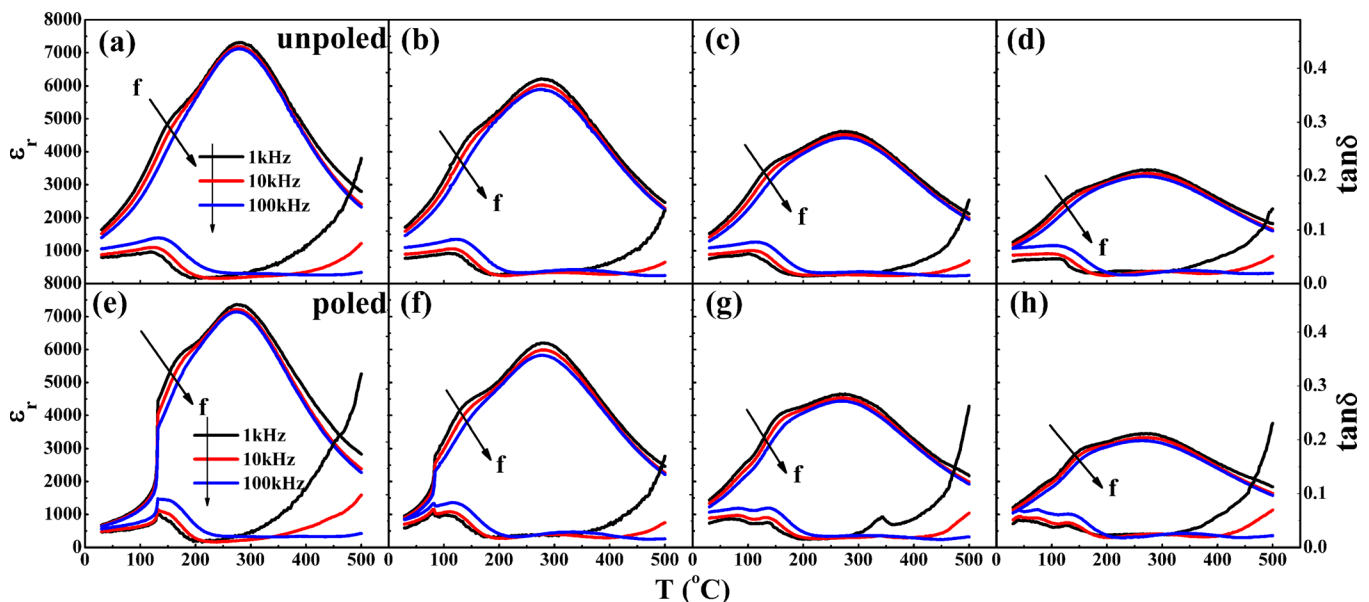


FIG. 4. The temperature dependent relative dielectric constant (ϵ_r) and dielectric loss ($\tan \delta$) for poled Sn-doped BNKT ceramics. The Sn content x was (a) 0, (b) 0.02, (c) 0.05, and (d) 0.08, respectively.

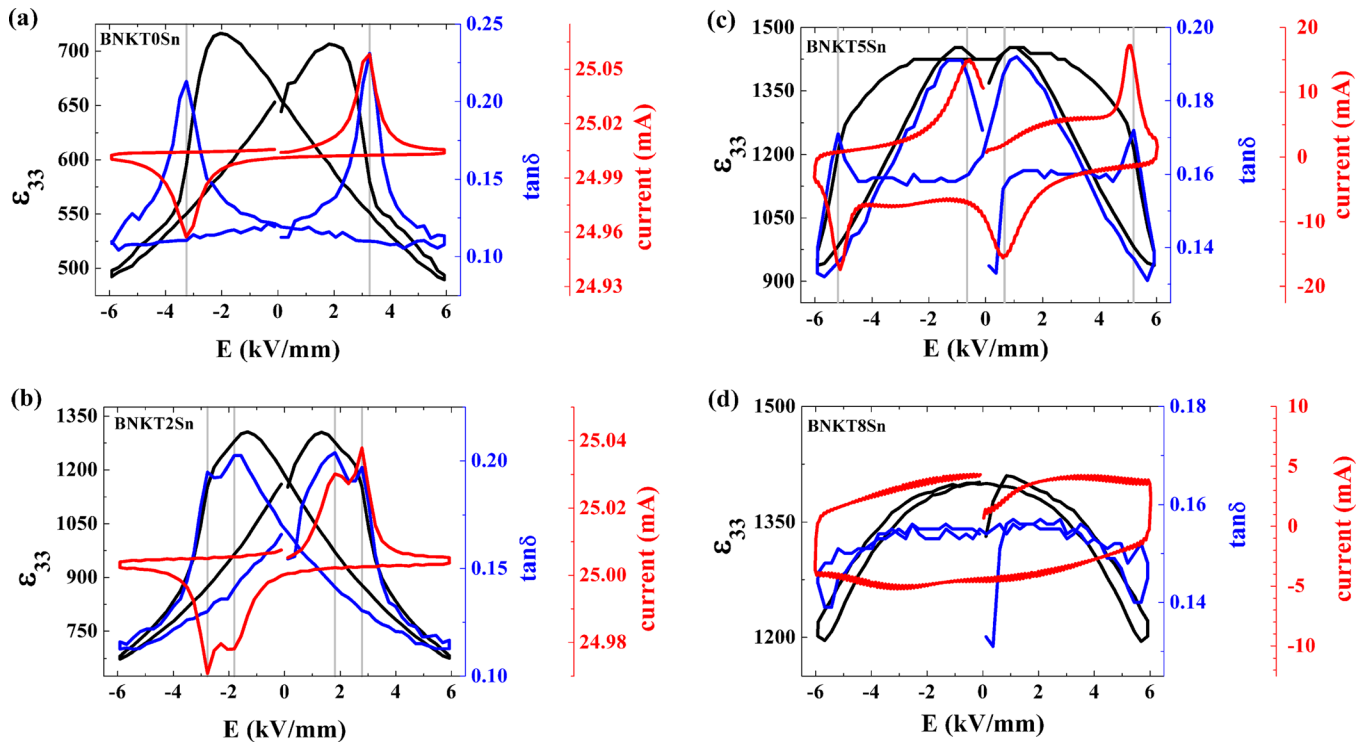


FIG. 6. Dielectric signals in comparison with the current flow during polarization reversal of BNKT_xSn.

of which gradually diffuse away with a further increase in Sn content.

Figure 6 presents the dielectric signals in comparison with the current flow during polarization reversal of BNKT_xSn. In the case of BNKT0Sn as in Fig. 6(a), it is seen that the dielectric loss peaks at the inflection point in dielectric permittivity, which corresponds to the coercive field where the switching current peaks. This single switching behavior implies that BNKT0Sn is fully converted into a FE phase during the electrical cycles. On the other hand, it is noted that the addition of 2 at. % Sn introduces a change in the switching behavior featured by a peak splitting in all the signals presented. Given the fact that this specific composition exhibits a trace of constriction in $P(E)$ as shown previously in Fig. 2(a), it is believed that the additional peak in the switching current reflects two-step switching, i.e., a dissociation of long-range FE domains prior to polarization reversal due to a compositionally induced instability of the field-induced FE order. It is noticed that this compositionally induced two-step switching behavior is in close phenomenological proximity to the thermally induced two-step switching behavior as proposed in a canonical relaxor $(\text{Pb}_{0.92}\text{La}_{0.08})(\text{Zr}_{0.65}\text{Ti}_{0.35})\text{O}_3$ (PLZT) near its depolarization temperature.^{33,34} The two-step switching hypothesis is, in fact, strongly supported by the data collected from BNKT0.05Sn and BNKT0.08Sn depicted, respectively, in Figs. 6(c) and 6(d). The field level required for the polarization reversal (E_{pr}) increases from ~ 3 kV/mm in BNKT0.02Sn to ~ 5 kV/mm in BNKT0.05Sn and so does the field for the dissociation of the field-induced long-range order (E_{dis}) from ~ 1.8 kV/mm in BNKT0.02Sn to ~ 0.7 kV/mm in BNKT0.05Sn. No peak in the switching current is evident in the case of BNKT0.08Sn, suggesting that the applied E_{max} of 6 kV/mm is not enough to induce a long-range ferroelectric

order, and thus there exists no long-range order to be defragmented for the successive cycles.

An emphasis is placed on the fact that E_{dis} becomes positive, which coincides with the appearance of giant strain, when the Sn content is increased from 2 to 5 at. %. The positive E_{dis} means that the field-induced FE order is not sustainable in the absence of bias field, confirming that the observed giant strain originates from incipient piezoelectricity.¹⁵ It is noticed that the giant strain due to the incipient piezoelectricity is a consequence of a repetitive reversible phase transition between a macroscopically “weakly” polar to a polar phase during each unipolar cycle.¹³ An insight into the nature of the macroscopically weakly polar phase may be grasped from the set of data collected from BNKT0.08Sn, since the field-induced phase transition is absent in this composition. In spite of the absence of a long-range polar order as evidenced from Fig. 6(d), it is seen that a significant d_{33} value (Figure 7) can be induced by the application of electric

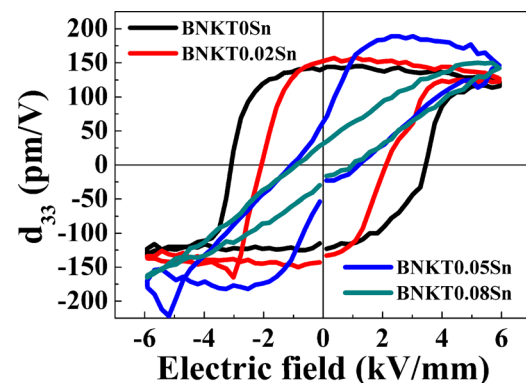


FIG. 7. Small signal $d_{33}(E)$ as a function of electric field.

fields. Considering the fact that this d_{33} value is largely based on the reversible contributions,^{33,35} this assumed macroscopically weakly polar phase is, in fact, microscopically strongly polar, and the individual polar vector of each polar entity is rather easily aligned and randomized in the presence and absence of a small electric field, respectively. Another important aspect of this macroscopically polar phase is revealed by Fig. 8(a) that depicts the S - P^2 of BNKT0.08Sn at room temperature. A strongly linear dependence of strain on polarization square is noted, classifying the observed strain in BNKT0.08Sn as a phenomenologically electrostrictive one. The phenomenological electrostrictive coefficient Q_{11} is estimated at $0.023 \text{ m}^4 \text{ C}^{-2}$, which is no smaller than that of the representative electrostrictive materials in the literature.³⁶ As commonly expected,^{19,37} both the electrostrictive coefficient and the strain are highly stable against temperature change (Fig. 8(b)). It follows that the macroscopically weakly polar phase can be defined as an ergodic relaxor ferroelectric composed of electrically sensitive mobile PNRs and the way the PNRs respond to the external electric fields is well described by phenomenological electrostrictive model.

Figure 9 presents $S_{\text{max}}/E_{\text{max}}$ of all the studied compositions as a function of temperature. Consistent with the earlier studies in BNT-based materials,^{19,38} $S_{\text{max}}/E_{\text{max}}$ of both BNKT0Sn and BNKT0.02Sn show a strong temperature dependence with a peak at a temperature near the depolarization temperature of each composition. It is known that the presence of peak in the $S_{\text{max}}/E_{\text{max}}$ originates from an enhancement in strain with the reduction in the remanent

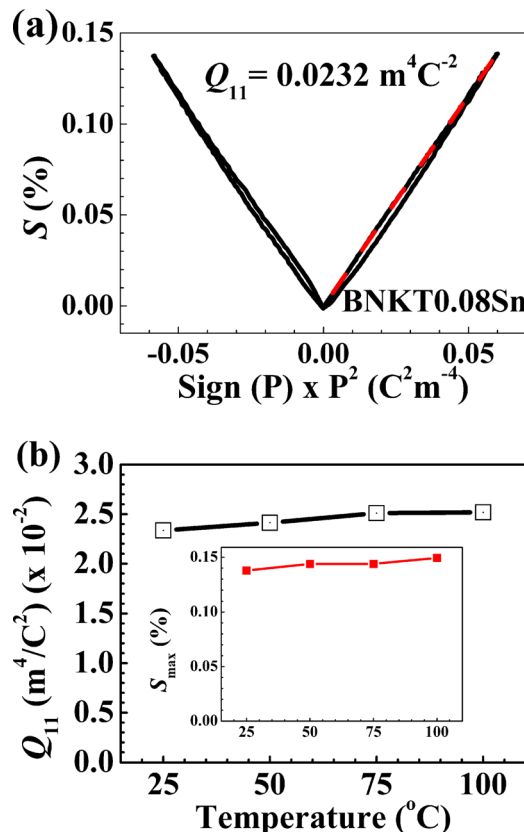


FIG. 8. Electric field-induced strain behavior of BNKT0.08Sn specimen: (a) S - P^2 plot and (b) temperature dependence of the electrostrictive coefficient and the electric field-induced strain (the inset).

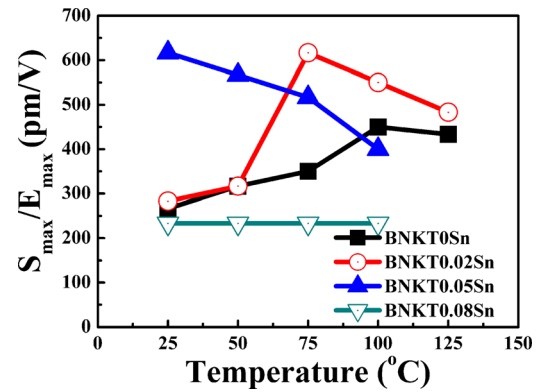


FIG. 9. $S_{\text{max}}/E_{\text{max}}$ of BNKT x Sn as a function of temperature.

strain of which results from the destabilization of field-induced long-range FE order.^{13,15} In this sense, the monotonic decrease of $S_{\text{max}}/E_{\text{max}}$ in BNKT0.05Sn in the absence of a peak in $S_{\text{max}}/E_{\text{max}}$ can be rationalized by the fact that the depolarization temperature is already below the room temperature. However, a comparison of the temperature coefficient of $S_{\text{max}}/E_{\text{max}}$ of BNKT0.05Sn with that of a previously reported 92BNT-6BT-2KNN featured by about $\sim 0.38\%/^{\circ}\text{C}$ change in $S_{\text{max}}/E_{\text{max}}$ up to 100°C reveals a significant decrease in temperature stability of BNKT0.05Sn at $\sim 0.72\%/^{\circ}\text{C}$. The reason for this deteriorated temperature stability is considered to be due to a highly diffused E_{pol} of BNKT0.05Sn, making the major contribution to $S_{\text{max}}/E_{\text{max}}$ over the studied temperature range rely largely on the field-induced phase transition that is, in general, highly sensitive to temperature changes. The current results suggest that tuning E_{pol} is one of the critical parameters in achieving practically important strains in incipient piezoceramics.

IV. CONCLUSIONS

The electric field-induced strain properties of Sn-doped BNKT solid solutions have been investigated by measuring $S(E)$, $P(E)$, XRD, small signal $d_{33}(E)$ and $\epsilon_{33}(E)$, and temperature-dependent dielectric permittivity spectra. Undoped BNKT showed typical FE features with significant P_r and E_c as well as butterfly-shaped S - E loops after electrical poling. As Sn-doping level increased to 5 at. %, a transition to an ergodic relaxor behavior was evidenced by a strong frequency-dependent dispersion in the dielectric permittivity and the appearance of a giant strain with a constriction in $P(E)$. Small signal $d_{33}(E)$ and $\epsilon_{33}(E)$ data confirmed that the observed giant strain originates from incipient piezoelectricity. Temperature dependence of the observed giant strain suggests that the slope of $P(E)$ at the poling field may play a critical role on temperature dependence of the giant strain. With a high Sn doping level of 8 mol. %, BNKT was demonstrated as a promising electrostrictive actuator application with a salient electrostrictive coefficient (Q_{11}) of $0.023 \text{ m}^4 \text{ C}^{-2}$.

ACKNOWLEDGMENTS

This work was supported by the National Research Foundation of Korea (NRF) Grant (2012K1A2B1A03000668). W. Jo sincerely thanks J. Rödel for careful proofreading and

comments. W. Jo acknowledges the financial support from the Deutsche Forschungsgemeinschaft (DFG) under SFB 595/A1 project.

- ¹T. R. Shrout and S. J. Zhang, *J. Electroceram.* **19**, 113–126 (2007).
- ²J. Rödel, W. Jo, K. T. P. Seifert, E. M. Anton, T. Granzow, and D. Damjanovic, *J. Am. Ceram. Soc.* **92**, 1153–1177 (2009).
- ³S. T. Zhang, A. B. Kounga, E. Aulbach, H. Ehrenberg, and J. Rödel, *J. Appl. Phys. Lett.* **91**, 112906 (2007).
- ⁴A. Hussain, C. W. Ahn, J. S. Lee, A. Ullah, and I. W. Kim, *Sens. Actuators A* **158**, 84–89 (2010).
- ⁵A. Hussain, C. W. Ahn, A. Ullah, J. S. Lee, and I. W. Kim, *Jpn. J. Appl. Phys., Part 1* **49**, 041504 (2010).
- ⁶K. N. Pham, H. B. Lee, H. S. Han, J. K. Kang, and J. S. Lee, *J. Korean Phys. Soc.* **60**, 207–211 (2012).
- ⁷N. B. Do, H. B. Lee, C. H. Yoon, J. K. Kang, and J. S. Lee, *Trans. Electr. Electron. Mater.* **12**, 64–67 (2011).
- ⁸E. A. Patterson, D. P. Cann, J. Pokorny, and I. M. Reaney, *J. Appl. Phys.* **111**, 094105 (2012).
- ⁹I.-K. Hong, H.-S. Han, C.-H. Yoon, H.-N. Ji, W.-P. Tai, and J.-S. Lee, “Strain enhancement in lead-free $\text{Bi}_{0.5}(\text{Na}_{0.78}\text{K}_{0.22})_{0.5}\text{TiO}_3$ ceramics by CaZrO_3 substitution,” *J. Intell. Mater. Syst. Struct.* (published online).
- ¹⁰V. D. N. Tran, A. Hussain, H.-S. Han, T. H. Dinh, J.-S. Lee, C.-W. Ahn, and I.-W. Kim, *Jpn. J. Appl. Phys.* **51**, 09MD02 (2012).
- ¹¹A. Sasaki, T. Chiba, Y. Mamiyal, and E. Otsuki, *Jpn. J. Appl. Phys., Part 1* **38**, 5564–5567 (1999).
- ¹²T. Takenaka, K. Maruyama, and K. Sakata, *Jpn. J. Appl. Phys., Part 1* **30**, 2236–2239 (1991).
- ¹³W. Jo, T. Granzow, E. Aulbach, J. Rödel, and D. Damjanovic, *J. Appl. Phys.* **105**(9), 094102 (2009).
- ¹⁴W. Jo, E. Erdem, R. A. Eichel, J. Glaum, T. Granzow, D. Damjanovic, and J. Rödel, *J. Appl. Phys.* **108**(1), 014110 (2010).
- ¹⁵W. Jo, R. Dittmer, M. Acosta, J. Zang, C. Groh, E. Sapper, K. Wang, and J. Rödel, *J. Electroceram.* **29**(1), 71–93 (2012).
- ¹⁶K. Uchino, “Piezoelectric actuators and ultrasonic motors,” in *Electronic Materials: Science and Technology*, edited by H. L. Tuller (Kluwer Academic Publishers, Boston, 1997).
- ¹⁷K. Wang, A. Hussain, W. Jo, and J. Rödel, *J. Am. Ceram. Soc.* **95**(7), 2241–2247 (2012).
- ¹⁸Y. Guo, M. Gu, H. Luo, Y. Liu, and R. L. Withers, *Phys. Rev. B* **83**(5), 054118 (2011).
- ¹⁹V. D. N. Tran, H. S. Han, C. H. Yoon, J. S. Lee, W. Jo, and J. Rödel, *Mater. Lett.* **65**, 2607–2609 (2011).
- ²⁰H. S. Han, C. W. Ahn, I. W. Kim, A. Hussain, and J. S. Lee, *Mater. Lett.* **70**, 98–100 (2012).
- ²¹Y. Hiruma, K. Yoshii, H. Nagata, and T. Takenaka, *J. Appl. Phys.* **103**, 084121 (2008).
- ²²N. Yasuda, H. Ohwa, and S. Asano, *Jpn. J. Appl. Phys., Part 1* **35**, 5099–5103 (1996).
- ²³C. C. Huang, D. P. Cann, X. Tan, and N. Vittayakorn, *J. Appl. Phys.* **102**, 044103 (2007).
- ²⁴T. Strathdee, L. Luisman, A. Feteira, and K. Reichmann, *J. Am. Ceram. Soc.* **94**(8), 2292–2295 (2011).
- ²⁵V. Q. Nguyen, H. S. Han, K. J. Kim, D. D. Dang, K. K. Ahn, and J. S. Lee, *J. Alloys Compd.* **511**, 237–241 (2012).
- ²⁶S. T. Zhang, A. B. Kounga, E. Aulbach, T. Granzow, W. Jo, H. J. Kleebe, and J. Rödel, *J. Appl. Phys.* **103**, 034107 (2008).
- ²⁷R. Dittmer, W. Jo, D. Damjanovic, and J. Rödel, *J. Appl. Phys.* **109**(3), 034107 (2011).
- ²⁸R. Dittmer, E. M. Anton, W. Jo, H. Simons, J. E. Daniels, M. Hoffman, J. Pokorny, I. M. Reaney, J. Rödel, and D. Damjanovic, *J. Am. Ceram. Soc.* **95**(11), 3519–3524 (2012).
- ²⁹H. S. Han, W. Jo, J. Rödel, I. K. Hong, W. P. Tai, and J. S. Lee, *J. Phys.: Condens. Matter.* **24**(36), 365901 (2012).
- ³⁰R. Dittmer, W. Jo, J. Daniels, S. Schaab, and J. Rödel, *J. Am. Ceram. Soc.* **94**, 4283–4290 (2011).
- ³¹Y. Zhang, D. C. Lupascu, E. Aulbach, I. Baturin, A. Bell, and J. Rödel, *Acta Mater.* **53**, 2203–2213 (2005).
- ³²V. Bobnar, Z. Kutnjak, R. Pirc, and A. Levstik, *Phys. Rev. B* **60**(9), 6420–6427 (1999).
- ³³S. Schaab and T. Granzow, *Appl. Phys. Lett.* **97**(13), 132902 (2010).
- ³⁴Q. Tan and D. Viehland, *Phys. Rev. B* **53**(21), 14103 (1996).
- ³⁵D. A. Hall and P. J. Stevenson, *Ferroelectrics* **187**(1), 23–37 (1996).
- ³⁶S.-T. Zhang, A. B. Kounga, W. Jo, C. Jamin, K. Seifert, T. Granzow, J. Rödel, and D. Damjanovic, *Adv. Mater.* **21**(46), 4716–4720 (2009).
- ³⁷J. Kuwata, K. Uchino, and S. Nomura, *Jpn. J. Appl. Phys., Part 1* **19**(11), 2099–2103 (1980).
- ³⁸S. T. Zhang, A. B. Kounga, E. Aulbach, W. Jo, T. Granzow, H. Ehrenberg, and J. Rödel, *J. Appl. Phys.* **103**(3), 034108 (2008).